Available online at www.sciencedirect.com
SCIENCE DIRECT®
C. R. Physique 6 (2005) 1139–1147
COMPTES RENDUS PHYSIQUE
http://france.elsevier.com/direct/COMREN/

MCAO for very large telescopes/OAMC pour les très grands télescopes

Multi-conjugate solar adaptive optics at the Vacuum Tower Telescope on Tenerife

Oskar von der Lühe *, Thomas Berkefeld, Dirk Soltau

Kiepenheuer-Institut für Sonnenphysik, Schöneckstr. 6-7, 79104 Freiburg, Germany

Available online 10 January 2006

Abstract

We present a breadboard multi-conjugate adaptive optics (MCAO) system for high angular resolution solar observations which we operate at the Vacuum Tower Telescope. We have developed methods to estimate quantitatively the performance of solar adaptive optics from science data. Several sets of short exposure images of the solar photosphere were analyzed to assess the performance of the MCAO. We demonstrate that a 30 arcsec field of view is substantially improved when the MCAO system is turned on. This compares favourably with an improvement of a 10 arcsec field with conventional solar adaptive optics. We also show how irradiance fluctuations in the MCAO compensated focus can be suppressed. ***To cite this article: O. von der Lühe et al., C. R. Physique 6 (2005).***

Résumé

Optique adaptative multi-conjugée avec le Vacuum Tower Telescope à Ténerife. Nous présentons un système d'optique adaptative multi-conjugée (OAMC) pour des observations solaires à haute résolution spatiale avec le Vacuum Tower Telescope (VTT). Nous avons dévelopé des techniques pour estimer les performances du système à partir des données scientifiques. On a analysé plusieurs séries d'images courte-pose pour évaluer l'apport de l'OAMC. On montre que le champ corrigé augmente à 30 arc secondes sitôt que l'OAMC est mise en marche, une amélioration bien importante par rapport à l'OA conventionelle. Nous montrons aussi comment les fluctuations d'illumination focale peuvent être supprimées. ***Pour citer cet article : O. von der Lühe et al., C. R. Physique 6 (2005).***

Keywords: Multi-conjugate adaptive optics; Solar observations

Mots-clés : Optique adaptative multi-conjuguée ; Observations solaires

1. Introduction

Adaptive optics (AO) is being operated on solar telescopes since a few years. Following the pioneering work at the National Solar Observatory (NSO) at Sacramento Peak, USA [1], there are now four regularly operating AO systems operating at the Dunn solar telescope of NSO, the 1 m Swedish Vacuum Telescope (SVT) in La Palma, Canaries Islands [2], at Big Bear

* Corresponding author.
E-mail addresses: ovdluhe@kis.uni-freiburg.de (O. von der Lühe), berke@kis.uni-freiburg.de (Th. Berkefeld), soltau@kis.uni-freiburg.de (D. Soltau).

1631-0705/$ – see front matter
doi:10.1016/j.crhy.2005.09.007

Solar Observatory (BBSO) [3], California, USA, and at the Vacuum Tower Telescope (VTT) of the Kiepenheuer-Institut für Sonnenphysik (KIS) in Tenerife, Canaries Islands [4,5]. At this time, only NSO and KIS work on the development of multi-conjugate adaptive optics for solar observations. The development at NSO are covered by several publications by Langlois and coauthors [6–8]. We describe recent results of the work done by us at the VTT in Tenerife.

The Sun is the only star which we can resolve to study fundamental processes of stellar physics at physically relevant scales—where they occur. The lower limit of observable structures on the solar surface are set by magneto-hydrodynamical processes in the photosphere, involving a highly structured magnetic field embedded in a plasma which exhibits complex motions at very small scales. Radiative transfer processes tend to 'blur' the radiation by scattering, however, the photon mean free path is of the order of 50 km at photospheric level and in many cases, variations of the source function may give rise to observable intensity fluctuations at considerably smaller scales. Present meter-class ground-based telescopes resolve about 100 km on the solar surface at their diffraction limit, setting the resolution limit in the vicinity of physically relevant scales. Solar physicists in Europe and in the US seek to improve substantially the resolution of solar observations, by building large aperture facilities, like the 1.5 m Gregor telescope on Tenerife [9] or the 4 m Advanced Technology Solar Telescope (ATST) of NSO [10].

On the other hand, solar scenes of interest are complex and dynamic, and extend over large fields. Fig. 1 shows two broadband images of typical active regions in the solar photosphere, covering a field of about one arcmin side length, which demonstrate the richness of small features close to the diffraction limit of the VTT.

A multi-conjugate adaptive optics system would compensate extended fields, enabling high resolution solar research with virtually any post-focus instrument, and permitting the full power of solar research and analysis tools to be applied. Given a sufficiently powerful adaptive optics system, large solar telescopes would provide observations with a spatial resolution which could never be achieved with any conceivable space telescope. This prospect is our motivation for developing MCAO. Solar research is excellently suited for multi-conjugate adaptive optics because the sun is extended and displays small scale structure everywhere on its surface. There is a 'natural guide star' wherever you point! Multi-directional wavefront sensing is therefore easy, making solar observations an ideal test bed for MCAO designs.

We have developed an extension to our conventional adaptive optics system KAOS [12] to study designs of MCAO for solar telescopes. KAOS is an integral part of the telescope and serves all post-focus instruments of the VTT. The extension is located in an optics lab near the science focus and therefore behaves like a separate instrument, with a set of cameras as the only science instrument. The purpose of the extension is to test various configurations of MCAO components together with the existing adaptive optics, in order to understand the control issues involved with MCAO, to test the limitations of various components and devices, and to develop the control software in a realistic situation at the telescope. We cannot afford a separate laboratory setup because of limited manpower and technical resources, and we have also made the experience that early tests

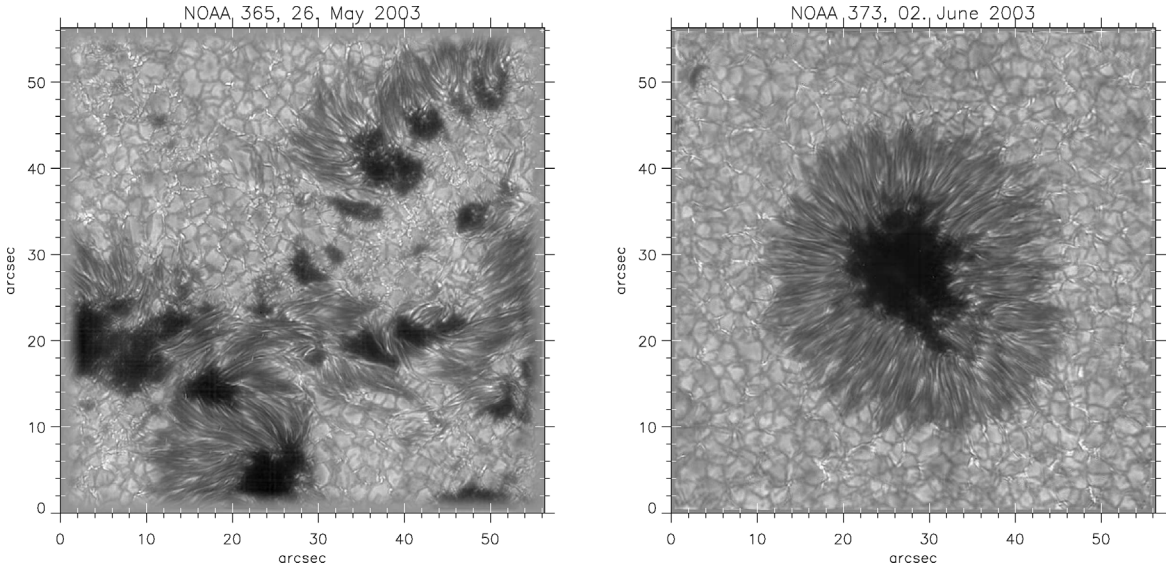

Fig. 1. High resolution images of the active regions NOAA 10365 and NOAA 10373 which appeared near the center of the solar disk in 2003. The images were obtained from sets of short exposures, taken in the Fraunhofer G band (430.5 nm) with partial adaptive optics compensation, and have been post-processed using a speckle imaging algorithm [11]. The spatial resolution approaches that of the 70 cm VTT at 430 nm which corresponds to 0.127 arcsec, or to about 100 km on the solar surface.

at the telescope help understanding where the real problems will be. However, the conditions at the VTT are too limited to consider any permanent MCAO installation other than the breadboard extension. Therefore, the current system has limitations, in particular in terms of system bandwidth. The ultimate goal of this effort is to specify and design an MCAO system for the new 1.5 m solar telescope Gregor which is under construction next to the VTT. We describe our MCAO system and present sample results in this article.

2. Description of the MCAO system at the VTT

Fig. 2 shows the configuration of the MCAO test setup at the VTT. The conventional adaptive optics system consists of a deformable and a tip-tilt mirror integrated in the telescope's optical path ('DM 1' in Fig. 2), a Hartmann–Shack wavefront sensor, and a computer where the control loop algorithms and the user interface are implemented. The MCAO extension consists of a second deformable mirror and a second wavefront sensor, both of which are connected to the control computer of the conventional AO. For the operation of the MCAO, a folding mirror is inserted just in front of the conventional science focus. A lens reproduces the focal plane with a scale that is adapted to the geometry of the second deformable mirror (DM 2). DM 2 is placed on a movable stage just behind the transferred focus, in a location whose conjugate corresponds to a distance between 11 to 14 km sunwards from the telescope. This range matches the distance of high altitude turbulence when observing the sun in the morning, with a zenith angle of some 45 degrees.

2.1. Wave front sensors

Both wavefront sensors can be used either separately or jointly. The first sensor (WFS 1) is used with the conventional AO. Its lenslet array has seven lenslets across the pupil diameter, corresponding to a subaperture diameter of 10 cm; cf. Fig. 3, right side. The central subaperture is always obstructed; edges of the pupil may be obscured as well in the morning or evening, depending on the orientation of the telescope's coelostat mirrors. The number of illuminated subapertures varies between 30 and 36. The image plane subfields on the detector cover 12 arcsec, limited by a field stop in front of the lenslet array. The wavefront error signal is produced by a comparison algorithm (FFT based cross correlation) of one of the subfields with each other one, resulting in up to 36 cross correlations or up to 72 X and Y shift values. The images are captured with a DALSA CA-D6 260 by 260 pixel camera which produces 960 frames/s and transferred via a PCI frame grabber board directly into the memory of the control computer. WFS 1 is capable of sensing more than 28 modes of wavefront deformation and performs as narrow-field high order sensor.

The second wavefront sensor (WFS 2) has only three subapertures across the pupil, amounting to a total of seven (left side of Fig. 3). The field of view covered by its detector—the same camera as for WFS 1—is some 40 arcsec to the side in each of the seven subapertures. Each of the seven sensor fields is divided into up to 19 overlapping, square areas which are 12 arcsec to the side. A cross correlation of corresponding areas for different subpupils provides the field dependent wavefront error signals (see upper left panel in Fig. 3). There is a total of up to 133 cross correlations per camera readout, resulting in up to 266 image shift values. WFS 2 can detect only few modes of wavefront deformation, up to 2nd radial order, and performs as wide-field low-order sensor. When used alone, WFS 2 is operated with the full rate of 960 frames per second, when used together with

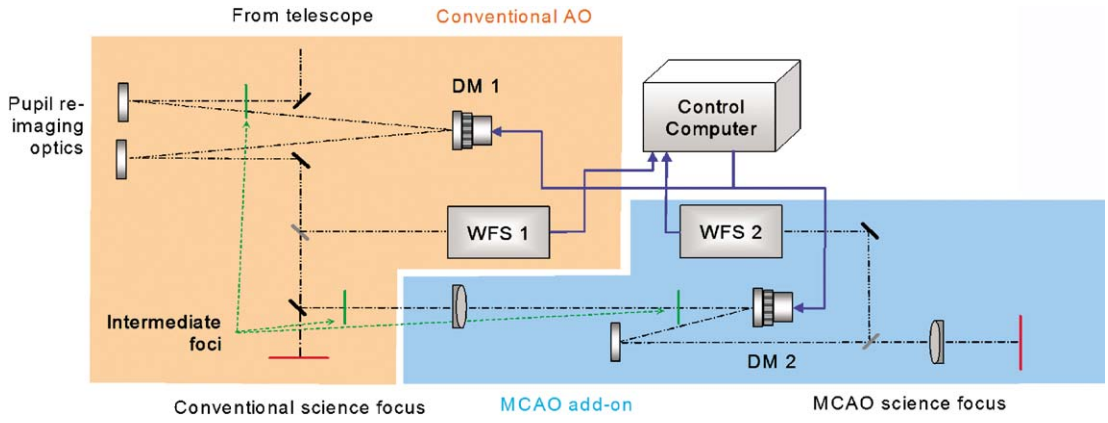

Fig. 2. Setup of the MCAO test bed at the VTT.

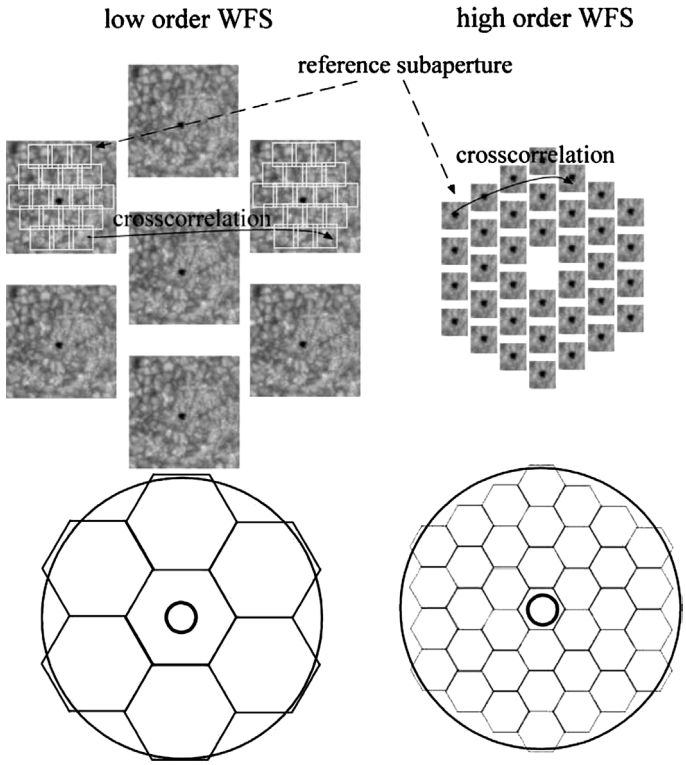

Fig. 3. Configuration of the two wavefront sensors.

WFS 1, the rate is reduced to 240 frames per second. In the latter configuration, the control loop bandwidth is limited to some 20 Hz.

2.2. Deformable mirrors

Deformable mirror 1 is a 50 mm diameter LaPlacian Optics bimorph mirror with 35 electrodes. We have used several devices for the second deformable mirror, including a second 35 electrode LaPlacian Optics bimorph mirror and a 37 electrode OKOTech MMDM with various degrees of success. Our current mirror is a 50 mm diameter 69 electrode bimorph mirror, fabricated to our specifications by *Night N* (*opt*) *Ltd.* [13] as prototype for the adaptive optics system of the 1.5 m Gregor telescope. The analog electronics including DAC and high voltage amplifiers are our own design, which has evolved from earlier developments in the area of fast tracking mirrors.

2.3. Control subsystem

The control algorithms and hardware management software have been developed for the conventional AO, keeping MCAO in mind, in order to make the migration between the setups as simple as possible. In general, the software is capable of handling any number of deformable mirrors and any number of wavefront sensors, the only limitation being computer hardware resources. All that it takes to switch from one setup to another one is to change parameter files. This flexibility allows us to change configurations with essentially no adjustments to the optical setup and only minimal manipulation of the control system, literally within minutes.

The control software runs essentially on any Unix-like operating system with a decent development environment. We are using the software under Solaris and Linux. The present control computer is a SunFire V880 equipped with eight 900 MHz processors.

2.4. Calibration and operation

The MCAO system is calibrated in several steps. First, an internal calibration of the wavefront sensors is performed by placing sun-illuminated pinholes at the positions of the WFS entrance field stops and by recording the zero position for each

Table 1
Operational modes of the MCAO test setup

Description	WFS 1	WFS 2	DM 1	DM 2	Loop rate [Hz]
Conventional AO	✓	–	✓	–	955
Ground-layer AO	–	✓	✓	–	955
Low-order MCAO	–	✓	✓	✓	955
High-order MCAO	✓	✓	✓	✓	240

subpupil. A single pinhole is used for the high-order sensor, a pattern of 19 pinhole on a slightly distorted hexagonal grid is used with the wide-field sensor. The guide regions on the solar surface are arranged in a slightly irregular hexagonal grid in order to prevent the buildup of waffle modes. Calibration needs to be repeated every several days, and each time a sensor is reconfigured.

Second, the whole control loop is calibrated. This step involves the 'poking' of each actuator of the system and recording the wavefront sensor responses from pinhole patterns, interspersed with relaxation of actuator hysteresis procedures. The wide-field sensor pinhole pattern must be identical to that used for the calibration of the wavefront sensor and must be carefully aligned. The reconstruction matrix is calculated using a truncated SVD on the interaction matrix, in the case of the low order MCAO separately for each mirror. Although not optimal, the field dependent (field differential) errors are essentially corrected by the high altitude DM (DM 2) while the field independent errors are corrected by the ground layer DM (DM 1).

This step needs to be repeated each time a reconfiguration of the system occurs, in particular a change of the number of illuminated subpupils. For good measure, this step is also repeated several times during the day to account for slow thermal creep. All essential mechanical functions are motorized and operate under computer control in a user-friendly fashion.

The calibration data are used to generate reconstructor matrices for various degrees of compensation with respect to system modes. The control system is capable to sense conditions of poor performance and automatically reduces the number of corrected modes if, e.g., the cross correlation becomes unstable in conditions of bad seeing. The control system increases the number of compensated modes when conditions improve. When the system loses lock entirely, the AO loop is opened and requires operator input to be closed again.

2.5. Operating modes

Table 1 lists the combinations of deformable mirrors and wavefront sensors which can be implemented with our setup.

Conventional adaptive optics combines the high-order wavefront sensor with the first DM, which is in a pupil plane conjugate. Ground-layer AO is implemented using the wide-field sensor in conjunction with the pupil plane deformable mirror. The calibration in this mode automatically results in a correction of wavefront deformations which are constant over the extended field. A low-order MCAO mode is implemented which uses the wide-field wavefront sensor alone with both DMs. We have restricted the number of fields within each subaperture of WFS 2 from 19 to 7—the central one and those at the edge positions of the outer hexagon—to increase the loop rate to the full 955 Hz in this mode.

The high-order MCAO configuration will be the normal mode of operation once the system is fully functional. It combines the measurements of the wide field sensor with the high-order wavefront sensor of the conventional AO to sense and correct the ground layer turbulence with better resolution than the wide field sensor would be able to do alone (36 versus seven subapertures). Furthermore, all 19 guiding regions of the wide field sensor will be used. The high-order wavefront sensor precedes the second deformable mirror and does not participate in its control because it is part of the conventional AO. This configuration is less than optimal for the operation of MCAO, but we found that it does not prevent, in principle, closing the loop with the full configuration.

3. MCAO tests and performance

We have performed extensive development tests of the MCAO system at the telescope during the past three years, establishing the first closed loop operation in May 2003 [14]. Most of the time was spent to debug hard- and software and to understand the 'real-world' problems of MCAO control, as well as to test various combinations of optical and electronic hardware. Since the MCAO system is based on the conventional AO which is in everyday use at the VTT, there has been no option other than spending most of the development work on site. It has also been our experience when developing the conventional AO system that many problems can only be properly assessed at the telescope. All in all, MCAO is probably an order of magnitude more complex than conventional AO.

3.1. Demonstration of low-order MCAO at the VTT

Most of the results presented in this section were obtained during an observation campaign in April 2005. The basic data are sequences of short exposure images of the compensated field, which are subject to a statistical analysis. We took images of the quiet sun near disk center in the G band (430.5 nm) with a Dalsa CA-D7 1024 by 1024 pixel camera, operating with a sustained frame rate of 10 s^{-1}, and delivering 10 ms exposures. Images were taken in bursts of 100 to 1000 frames and stored on hard disk for later processing.

We present the results of analyses of short exposure bursts, taken within half an hour on April 24, and representing the operating modes of conventional AO and low-order MCAO, as well as operation without adaptive optics. The conventional AO data set consisting of 100 frames has been taken first. Only WFS 1, DM 1 and the tip-tilt mirror were operated. WFS1 measured a single guiding region on the Sun with 36 subapertures. The loop rate was 955 Hz. Both MCAO and 'no AO' sets include 200 frames which belong to the same 1000 frame burst during which the control loop was opened. The two sets are taken within 80 s from each other, 30 min after the first set. Only WFS 2 was operated, using 7 subapertures and 7 guiding regions on the Sun (cf. Section 2.5), but both deformable mirrors as well as the tip-tilt mirror were controlled. The loop rate was again 955 Hz. Seeing has been judged fair during the entire period. Only 7 to 15 modes were used to correct the ground seeing. 5 modes were used to correct the off-axis errors induced by the high altitude turbulence.

Since there are no stable point sources, the judgement of the performance of a solar adaptive optics system is generally difficult. Solar small scale structure evolves over time scales of a few minutes; quiet sun granulation has an intrinsic contrast of some 12% and a power spectrum which peaks at scales between 1 and 2 arcsec. We have developed several indicators to quantify performance of solar AO which we present here.

One quality indicator is the contrast of a long exposure image. Fig. 4 presents the average images of the three bursts. The improvement of image quality when the adaptive optics is turned on is evident. The average image with the AO turned off lacks small scale detail and has a contrast of 3.8% which to our experience is typical for '2 arcsecondish' seeing. The image improves considerably across the field with conventional AO. The wide field effect is mostly caused by the compensation of image motion which remains correlated over a larger field angle, other causes for improvement are reduction of instrumental aberrations and compensation of ground layer turbulence. The granulation is sharper, compared to the edge of the field, at the lock point close to the center. This is caused by the expected anisoplanatism, which limits the best compensated field to a patch of about 10 arcsec in diameter with a center at (25, 20) arcsec. The contrast, computed over the entire field, increases to 4.4%. The compensated field is considerably larger, covering roughly 30 arcsec in diameter, when the MCAO is turned on, demonstrating its expected performance. Again, the center of the compensated field is somewhat below the center of the frame. The overall contrast is 5.6%, corresponding to 'sub-arcsecondish' seeing. We have analyzed several sets of data in addition to the ones presented here, taken with various modes of the MCAO system, all showing the same general behaviour where the improved field increases to some 30 arcsec as soon as the multi-conjugate mode is operating. A noticeable improvement of image quality without reaching the diffraction limit, as demonstrated here, is typical for the partial compensation that our system is capable to deliver under the seeing conditions present at the time of observation.

Further analysis of the bursts involves measurements of differential image motion by correlation tracking of small sections of the field of view. We have divided the original bursts into series of 6 arcsec subfields (1/8 of the frame size) which overlap by half of their width and height. The result is the residual image motion as a function of field angle, on a square raster of 15 by 15 positions, 3 arcsec apart. Fig. 5 shows the results. There is significant homogeneous image jitter when AO is not operating (note the difference in the scale). The average rms position error across the field is 0.9 arcsec. The image motion is substantially reduced over all the field with conventional AO, but showing clearly a strong gradient from the lock point at position (26, 22) arcsec. The minimum rms image motion at the lockpoint is 0.07 arcsec, increasing to 0.35 arcsec near the edge of the field. Such a pattern is very typical for conventional AO. Evidently, the image-motion compensated field is considerably larger with MCAO. The rms value remains nearly constant at 0.08 arcsec within an area of 20 arcsec in diameter, increasing fairly steeply to 0.35 arcsec near the edge of the field. Again, such a behaviour is expected from MCAO where the compensation deteriorates rapidly beyond the sensed field of view.

Further evidence for the effectiveness of our MCAO system was obtained from speckle image reconstructions [11] performed on the bursts presented here. An essential step in the reconstruction process is the estimation of the Fried parameter r_0 which is needed for amplitude calibration [15]. For the case of partial adaptive optics compensated data, this estimate yields the generalised Fried parameter ρ_0 introduced by Cagigal et al. [16]. The estimate depends on the field angle because of anisoplanatism and makes field-dependent amplitude calibration of the speckle reconstruction necessary. The distribution of ρ_0 across the field for all three cases described here is shown in Fig. 6. Without adaptive optics, ρ_0 corresponds to r_0 and amounts to some 7 cm at 430 nm (8.4 cm at 500 nm), uniformly distributed across the field (the variation seen in the left panel of 6 gives an impression of the accuracy of the estimation). With conventional adaptive optics, there is a clear variation of ρ_0 across the field with a maximum of 10.5 cm (12.6 cm at 500 nm) at the lock point and degrading rapidly within 5 arcsec. The improved

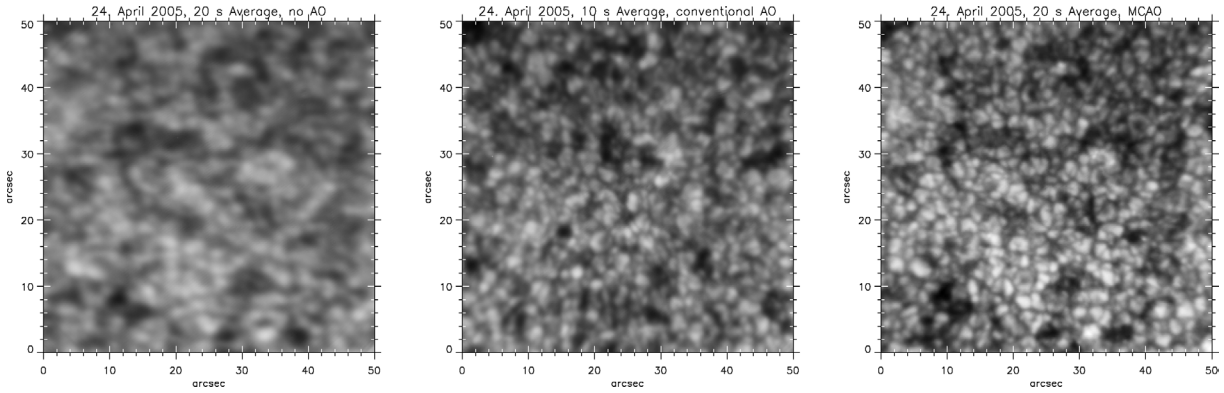

Fig. 4. Long exposure images of disk center quiet sun taken without adaptive optics (left), with conventional AO (middle) and with MCAO (right), shown on a common contrast scale. These images were generated by averaging 200 frames; 100 frames for the case of conventional AO. The full frame rms contrast of these images are 0.0375 (no AO), 0.0436 (conv. AO), and 0.0556 (MCAO) of the mean intensities.

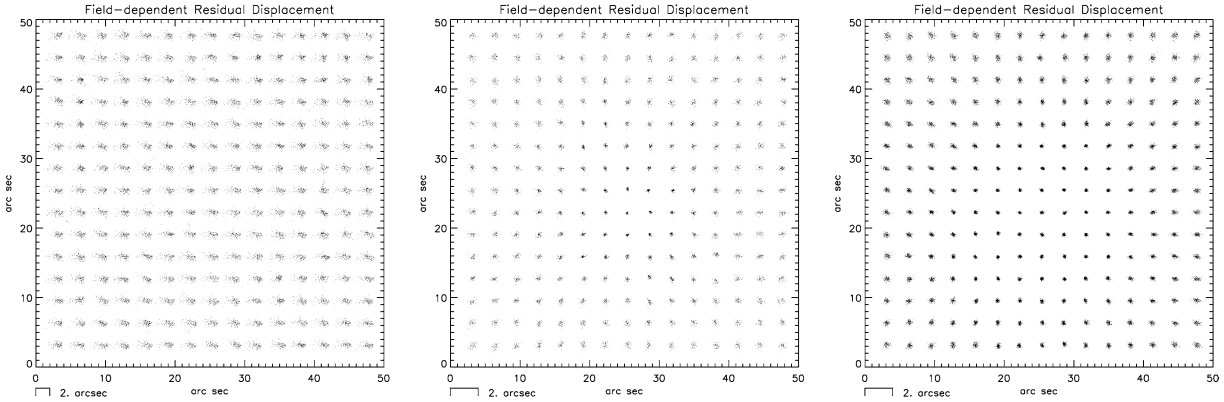

Fig. 5. Residual field-dependent image motion of the short exposure series of Fig. 4. Left: no AO, middle: conventional AO, right: MCAO. The estimated position errors are shown as spot clouds at the subfield center positions. The scale bar at the bottom applies to the spot clouds.

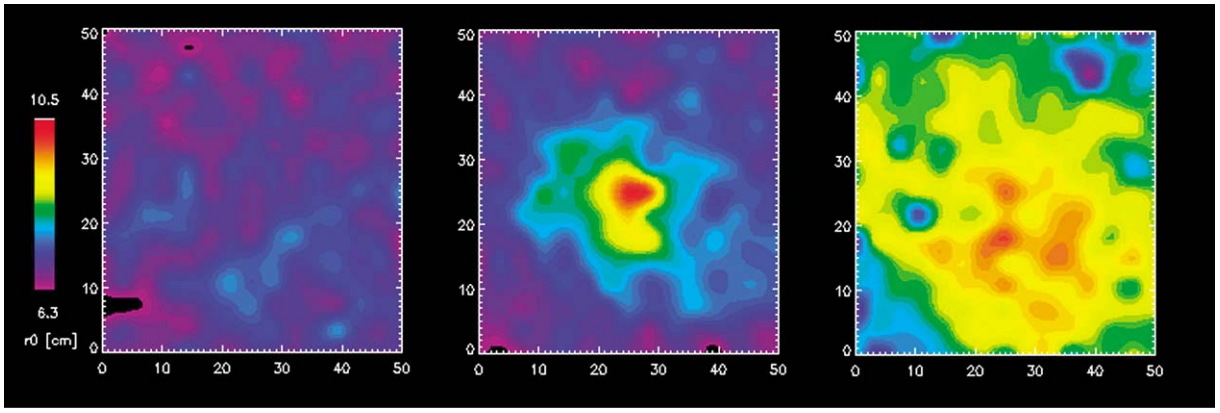

Fig. 6. Field dependence of generalized Fried parameter ρ_0. Left: no AO, middle: conventional AO, right: MCAO. The field sizes are given in arcsec.

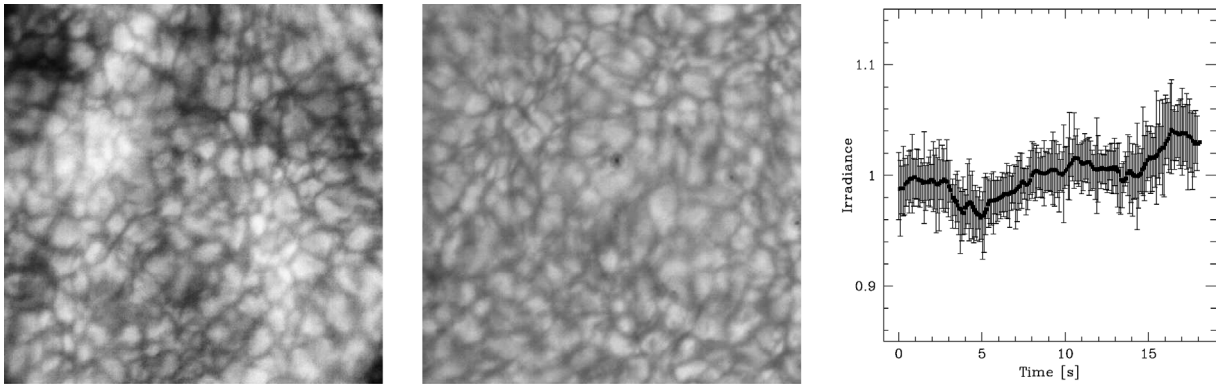

Fig. 7. Short exposures showing an MCAO compensated solar field. Left: irradiance fluctuations due to local curvature of the second DM. Center: irradiance fluctuations removed by a pupil stop in the camera branch. These images were taken during tests in November 2004. Right: mean intensity and minimum/maximum span of large scale intensity variations in the MCAO compensated data from 24 April 2005.

field extends over a much larger area with MCAO. The comparison is particularly striking considering that the data for MCAO and without AO were taken just about a minute apart in time.

3.2. Irradiance fluctuations

We have noted already in 2003 that MCAO produces rapid fluctuations of irradiance of a few percent in the compensated focal plane when observing the solar surface. These fluctuations are absent in the uncompensated focal plane, and apparently correlate with the local curvature of the deformable mirror in the plane conjugated to the high altitude turbulence layer. We were able to explain the fluctuations with the field dependent changes of effective focal length introduced by a high altitude layer and which is related to image distortion [15]. Using a simple geometric model of the MCAO system, we have reproduced in theory the observed irradiance effects.

We have proposed to insert a slightly undersized aperture stop at the location of the nominal exit pupil in order to remove the fluctuations in the compensated field. This supposition was confirmed during test runs in September and November 2004, when images have been taken with and without a pupil stop in the compensated science channel. Fig. 7 shows the irradiance effect and its absence when a pupil stop is inserted in the optical branch of the compensated camera channel. This test was undertaken to convince ourselves the viability of the pupil stop concept, but not under conditions which are representative for the operation of MCAO. We conclude that a pupil stop will be effective, but the exact conditions need to be further investigated. The graph in Fig. 7 shows the variation with time of maximum and minimum of the MCAO burst of Fig. 4, low-pass filtered to display only the fluctuation effect. The amplitude of the fluctuation amounts to a few percent of the mean intensity and depends on the axial position of the second DM; it becomes more prominent when the DM is closer to the focus, i.e., conjugate to a higher altitude.

4. Conclusion

We have operated multi-conjugate adaptive optics on extended fields of view when observing the solar surface with the Vacuum Tower Telescope in Tenerife. The MCAO system improves the image quality substantially compared to the attainable resolution under identical seeing conditions when the system is turned off. Compared to conventional adaptive optics, our MCAO system increases the size of the compensated field by a factor of three; this increase is consistent in all data sets investigated so far. There are indications that the conventional adaptive optics produces a better compensation at the lock point compared to MCAO. A possible cause might be differences in seeing quality during the collection of the compared data sets. A better performance of conventional AO compared with the low-order MCAO should be expected anyway, because the latter would at best compensate up to 9 modes of wavefront deformation. There is much more data waiting to be analyzed, which will help us putting the present results on firmer grounds.

The present setup is little more than a breadboard test. Its advantages are flexibility and the opportunity to test various optical configurations in a fairly painless and straightforward manner. Major shortcomings are the low number of modes which can be compensated and an as yet too low closed-loop bandwidth. The main purpose of the setup is to gain experience with MCAO, to demonstrate the viability of MCAO for solar observations, and to develop the required control environment to operate MCAO in a stable and user-friendly manner. These goals have been achieved to a large degree. The setup at the VTT—as well as the

general post-focus environment—is not suited to support MCAO, and the breadboard was never meant to become a user facility at the VTT.

We will use the experience gained to develop a much more powerful system for the 1.5 m Gregor telescope which is being constructed next to the VTT at this time.

Acknowledgements

We would like to thank Friedrich Wöger and Kasia Mikurda from the Kiepenheuer-Institut, and Markus Sailer from the Universitätssternwarte Göttingen for their skillful expertise and help in setting up the data recording equipment, for providing some of the images shown here, as well as for many fruitful discussions. Thomas Schelenz has been pivotal in getting the electronics built and debugging anything that is analog.

References

[1] T.R. Rimmele, R.R. Radick, Solar adaptive optics at NSO/SP, in: D. Bonaccini, R. Tyson (Eds.), Adaptive Optics System Technologies, in: Proc. SPIE, vol. 3353, 1998.
[2] G.B. Scharmer, Adaptive optics system for the new Swedish solar telescope, in: S.L. Keil, S.V. Avakyan (Eds.), Innovative Telescopes and Instrumentation for Solar Astrophysics, in: Proc. SPIE, vol. 4007, 2003, pp. 370–380.
[3] A. Tritschler, C. Denker, T. Rimmele, K. Richards, S. Hegwer, The high-order adaptive optics at the Big Bear Solar Observatory, Solar Phys. (2005), in preparation.
[4] D. Soltau, Th. Berkefeld, O. von der Lühe, F. Wöger, Th. Schelenz, Adaptive optics and multi-conjugate adaptive optics with the VTT, Astr. Notes 323 (2002) 236–240.
[5] O. von der Lühe, D. Soltau, Th. Berkefeld, Th. Schelenz, KAOS: adaptive optics system for the Vacuum Tower Telescope at Teide Observatory, in: S.L. Keil, S.V. Avakyan (Eds.), Innovative Telescopes and Instrumentation for Solar Astrophysics, in: Proc. SPIE, vol. 4853, 2003, pp. 187–193.
[6] M. Langlois, G. Moretto, K. Richards, S. Hegwer, Th. Rimmele, Solar multiconjugate adaptive optics at the Dunn Solar Telescope: preliminary results, in: D. Bonaccini, B. Ellerbroeck, R. Ragazzoni (Eds.), Advancements in Adaptive Optics, in: Proc. SPIE, vol. 5490, 2004, pp. 59–66.
[7] G. Moretto, M. Langlois, K. Richards, S. Hegwer, D. Gilliam, Th. Rimmele, Optical set-up and design for solar multiconjugate adaptive optics at Dunn Solar Telescope/NSO, in: D. Bonaccini, B. Ellerbroeck, R. Ragazzoni (Eds.), Advancements in Adaptive Optics, in: Proc. SPIE, vol. 5490, 2004, pp. 905–912.
[8] M. Langlois, G. Moretto, K. Richards, S. Hegwer, Th. Rimmele, Solar multi-conjugate adaptive optics closed loop at the Dunn Solar Telescope, in: Proceedings JSO ONERA, ONERA, Paris, 2005.
[9] R. Volkmer, O. von der Lühe, F. Kneer, J. Staude, T. Berkefeld, P. Caligari, W. Schmidt, D. Soltau, H. Nicklas, E. Wiehr, A. Wittmann, H. Balthasar, A. Hofmann, K. Strassmeier, M. Sobotka, M. Klvana, M. Collados, The new 1.5 solar telescope GREGOR: Progress report and results of performance tests, in: Solar Physics and Space Weather Instrumentation, in: Proc. SPIE, vol. 5901, 2005, in press.
[10] T.R. Rimmele, S. Keil, J. Wagner, N. Dalrymple, B. Goodrich, E. Hansen, F. Hill, R. Hubbard, L. Phelps, K. Richards, M. Warner, The ATST Team and the Site Survey Working Group, Advanced Technology Solar Telescope: A progress report, in: Solar Physics and Space Weather Instrumentation, in: Proc. SPIE, vol. 5901, 2005, in press.
[11] K. Mikurda, O. von der Lühe, High resolution solar speckle imaging with the extended Knox–Thompson algorithm, Solar Phys., 2005, submitted for publication.
[12] Th. Berkefeld, D. Soltau, O. von der Lühe, Multiconjugate adaptive optics at the Vacuum Tower Telescope, in: A. Kohnle, J.D. Gonglewski, Th. J. Schmugge (Eds.), Optics in Atmospheric Propagation and Adaptive Systems IV, in: Proc. SPIE, vol. 4538, 2001, pp. 119–127.
[13] V.V. Samarkin, A. Aleksandrov, A.V. Kudryashov, Semipassive bimorph correctors for multipurpose applications, in: P.L. Wizinowich, D. Bonaccini (Eds.), Adaptive Optical System Technologies II, in: Proc. SPIE, vol. 4839, 2003, pp. 741–749.
[14] O. von der Lühe, Photomeric stability of multi-conjugate adaptive optics, in: D. Bonaccini, B. Ellerbroeck, R. Ragazzoni, (Eds.), Advancements in Adaptive Optics, in: Proc. SPIE, vol. 5490, 2004, pp. 617–624.
[15] O. von der Lühe, A method to estimate Frieds parameter from a series of arbitrary structure, J. Opt. Soc. Amer. A 1 (1984) 741–755.
[16] M.P. Cagigal, V.F. Canales, Generalized Fried parameter after adaptive optics partial wave-front compensation, J. Opt. Soc. Amer. A 17 (5) (2000) 903–910.